

# Simple but Stronger UO, Double but Weaker UNMe

## Bonds: The Tale Told by Cp<sub>2</sub>UO and Cp<sub>2</sub>UNR.

Noémi Barros,<sup>a,b,c</sup> Daniel Maynaud,<sup>d</sup> Laurent Maron,<sup>a\*</sup> Odile Eisenstein,<sup>b\*</sup> Guofu Zi,<sup>e</sup> Richard A. Andersen.<sup>e</sup>

a) LPCNO, CNRS-UPS-INSA, INSA Toulouse, 137 avenue de Rangueil, 31077 Toulouse, France

b) Institut Charles Gerhardt, CNRS-UM2-ENSCM-UM1, CTMM, cc1501, Université Montpellier 2,

34095 Montpellier, France c) DEN/DRCP/SCPS/LCAM, CEA Valrhô, BP 17171, 30207 Bagnol-

sur-Cèze cedex, France d) Laboratoire de Chimie et Physique Quantiques, CNRS, IRSAMC,

Université Paul Sabatier, 118 Route de Narbonne, 31064 Toulouse Cedex 04, France e) Chemistry

Department and Chemical Sciences Division of Lawrence Berkeley National Laboratory, University of California, Berkeley, California 94720.

**laurent.maron@irsamc.ups-tlse.fr odile.eisenstein@univ-montp2.fr**

**RECEIVED DATE (to be automatically inserted after your manuscript is accepted if required according to the journal that you are submitting your paper to)**

**ABSTRACT** The free energies of reaction and the activation energies are calculated, with DFT (B3PW91) and small RECP core potential for uranium, for the reaction of Cp<sub>2</sub>UNMe and Cp<sub>2</sub>UO with MeC≡CMe and H<sub>3</sub>SiCl that yields 1,2-cycloaddition and 1,2-addition products, respectively. CAS(2,7) and DFT calculations on Cp<sub>2</sub>UO and Cp<sub>2</sub>UNMe give similar results, which validates the use of DFT calculations in these cases. The calculated results mirror the experimental reaction of

[1,2,4-(CMe<sub>3</sub>)<sub>3</sub>C<sub>5</sub>H<sub>2</sub>]<sub>2</sub>UNMe with dimethylacetylene and [1,2,4-(CMe<sub>3</sub>)<sub>3</sub>C<sub>5</sub>H<sub>2</sub>]<sub>2</sub>UO with Me<sub>3</sub>SiCl. The net reactions are controlled by the change in free energy between the products and reactants, not by the activation energies, and therefore by the nature of the UO and UNMe bonds. A NBO analysis indicates that the U-O interaction is composed of a single U-O  $\sigma$  bond with three lone pairs of electrons localized on oxygen in Cp<sub>2</sub>UO leading to a polarized U-O fragment. In contrast, the U-NMe interaction in Cp<sub>2</sub>UNMe is composed of a  $\sigma$  and  $\pi$  component and a lone pair of electrons localized on the nitrogen, resulting in a less polarized UNMe fragment in accord with the lower electronegativity of NMe relative to O. The strongly polarized U<sup>(+)</sup>-O<sup>(-)</sup> bond is calculated to be about 71 kcal mol<sup>-1</sup> stronger than the less polarized U=NMe bond.

**Introduction** The synthesis and properties of the uranium metallocene derivatives Cp'<sub>2</sub>UX where Cp' is 1,2,4-tri-*t*-butylcyclopentadienyl, X is O or NR, (R is Me or 4-MeC<sub>6</sub>H<sub>4</sub>, 4-(MeO)C<sub>6</sub>H<sub>4</sub>, 4-(Me<sub>2</sub>N)C<sub>6</sub>H<sub>4</sub>, have been described.<sup>1,2</sup> The solid state structures of the Lewis base adduct of the oxo derivative Cp'<sub>2</sub>UO(4-(Me<sub>2</sub>N)C<sub>6</sub>H<sub>4</sub>N) and the base-free imido derivative Cp'<sub>2</sub>U(N-4-MeC<sub>6</sub>H<sub>4</sub>) show that these metallocenes are monomeric in the solid state. The oxo derivative is in equilibrium with the base-free metallocene in solution and base-free Cp'<sub>2</sub>UO was isolated and shown to be a monomer in the gas phase. In order to compare the chemical properties of the oxo and imido metallocenes, it was desirable to prepare imido derivatives in which the NR group is as sterically small as possible so that the electronic differences would be dominant. Although Cp'<sub>2</sub>UNH could not be prepared, the NMe derivative was isolated and shown to be a monomer in gas phase. Thus, an isoelectronic set of metallocenes that are as sterically similar as possible was available, so that their chemical and physical properties could be studied and compared.

These studies showed that the imido-metallocenes, R = Me, 4-MeC<sub>6</sub>H<sub>4</sub>, react with benzophenone rapidly and cleanly to give the oxo-metallocene and Ph<sub>2</sub>C=NR. This reaction showed that the bond dissociation enthalpy of UO was greater than that of UNR by the difference between C=O and

C=NR, which has been estimated to be at least 30 kcal mol<sup>-1</sup>.<sup>3</sup> Further, Cp'<sub>2</sub>UNMe, but not Cp'<sub>2</sub>UN(4-MeC<sub>6</sub>H<sub>4</sub>), yielded isolable azacyclobutene derivatives with dimethyl- and diphenylacetylene, which are intermediates in the catalytic hydroamination of di-substituted acetylenes.<sup>1,2,4</sup> In contrast, the oxometalocene did not react with either of these acetylenes, but Cp'<sub>2</sub>UO did react with an excess of Me<sub>3</sub>SiX reagents, such as Me<sub>3</sub>SiCl, to give Cp'<sub>2</sub>U(OSiMe<sub>3</sub>)Cl, however, the imidometalocenes, did not react with Me<sub>3</sub>SiCl.

The different reactivity pattern was suggested to result from the ground state electronic structure of the metallocenes, *viz.*, the double-bond resonance structure dominates the polar single bond resonance structure in Cp'<sub>2</sub>UNR while the converse is true in Cp'<sub>2</sub>UO. The reactivity difference can be justified by comparing the electron affinity of the isoelectronic fragments; the experimental gas phase electron affinity (in electron volts, eV) are: O (1.46 eV),<sup>5</sup> NPh (1.45 eV),<sup>6</sup> NH (0.38 eV),<sup>7</sup> and NMe (0.022 eV).<sup>8</sup> The electron affinity values of O and NMe reflect the relative electronegativities of the non-metal atoms, but substituent effects substantially change the electron affinity of the nitrene fragment.

In this article, DFT calculations on Cp<sub>2</sub>UO and Cp<sub>2</sub>UNMe, which are justified by multi-reference calculations, are reported. The calculations justify and extend the general correctness of the qualitative bond model advanced above. In particular, the calculations of the potential energy surfaces for the reactions of Cp<sub>2</sub>UO and Cp<sub>2</sub>UNMe with various organic molecules show that kinetic barriers are relatively low and the reactions are under thermodynamic control, but steric effects play a role in manipulating the activation energies in the reactions of the imidometalocenes.

## Results

### Strategy

Computational studies of compounds of the 5f block metals are still relatively rare and these studies are described in several recent reviews<sup>9</sup> and a database.<sup>10</sup> Calculations on these complexes of

the 5f block metal are rather challenging because of relativistic and correlation effects, involving the 5f electrons.<sup>11</sup> It is especially important to account for electron correlation in the case of energetically degenerated f shells but such calculations require extensive amounts of computational time and it is necessary to model the real systems in order to reduce the number of atoms and therefore the amount of computational time.<sup>12,13</sup> The DFT approach is attractive because it opens the possibility of calculating large species but the results should be handled with considerable caution since, by definition, DFT calculations cannot be used for highly multi-reference systems, that is, those systems that cannot be described by a single configuration, because they can lead to wrong conclusions about the electronic ground state of molecules, such as cerocene,<sup>14</sup> or to the heat of reaction, as in the case of the reduction of uranyl by dihydrogen.<sup>12</sup> However, it has been shown that the ground state molecular geometry is not sensitive to the f-electronic state<sup>15</sup> and DFT methods give optimized geometries in agreement with experiment.<sup>12,16</sup> Thus, DFT calculations should be validated by multi-reference calculations in the case of open shell systems such as the actinide metal complexes described in this article. Although uranyl complexes have been studied by computational methods,<sup>17</sup> these  $\text{UO}_2^{2+}$  species are different from those in this article. In addition, computational studies have been reported only recently on the nitrene analogues.<sup>18</sup>

The metallocenes used in the experimental study were  $[\eta^5\text{-}1,2,4\text{-(CMe}_3)_3\text{C}_5\text{H}_2]_2\text{UO}$  and  $[\eta^5\text{-}1,2,4\text{-(CMe}_3)_3\text{C}_5\text{H}_2]_2\text{UNMe}$ , and in the computational studies these complexes were replaced by  $(\text{C}_5\text{H}_5)_2\text{UO}$ , abbreviated as  $\text{Cp}_2\text{UO}$ , and  $(\text{C}_5\text{H}_5)_2\text{UNMe}$  abbreviated as  $\text{Cp}_2\text{UNMe}$ . The modeling of  $1,2,4\text{-(CMe}_3)_3\text{C}_5\text{H}_2$  by  $\text{C}_5\text{H}_5$  has been used for the computational studies of lanthanides complexes reported earlier. Substituents on the cyclopentadienyl rings certainly influence the spectroscopic properties in metallocene complexes, such as CO stretching frequencies in metallocene carbonyl compounds.<sup>19</sup> However, it is assumed that the relative free energies of the reactants, products, and transition states are reproduced correctly when  $\text{C}_5\text{H}_5$  replaces the substituted cyclopentadienyl ligands, that is, the trends in the relative energies along the potential energy surface are reliable,<sup>20</sup> unless steric effects dominate the electronic effects.

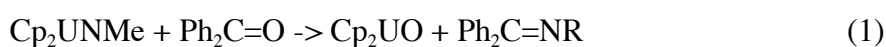
In this article, small core ECP calculations are performed on the uranium complexes in order to confirm that the DFT methods correctly reproduce the bond lengths and angles obtained in the experimental metallocenes. The metallocene described in this article have a  $5f^2$  electronic structure and thus are spin triplets above about 50K.<sup>21</sup> The triplet state, obtained at the DFT level of calculation, is confirmed by CASSCF calculations. The latter calculations also show that the triplet states do not exhibit significant multi-reference character and therefore justify the use of single configuration methodologies. Geometry optimizations at the CASSCF level also yield results in agreement with the DFT calculations.

The order of presentation is (a) the free energy of reaction for the reaction of  $Cp_2UNMe$  and  $Ph_2C=O$  to give  $Cp_2UO$  and  $Ph_2C=NMe$ , (b) the potential energy surface for the reaction of  $Cp_2UNMe$  with  $H_2C=O$  to give  $Cp_2UO$  and  $H_2C=NMe$  and (c) the potential energy surfaces for the reactions of  $Cp_2UNMe$  and  $Cp_2UO$  with  $MeC\equiv CMe$  and  $H_3SiCl$  are then described. This order of presentation is adopted since the free energy changes between the reactants and products are defined by the bonding in the  $UO$  and  $UNMe$  fragments, which leads naturally into a bond model for these fragments. All of the energies are reported as free energies ( $\Delta G$ ) to account for the change of molecularity in the reactions and these trends are verified by calculation of  $\Delta E$ .

## Results

### Reaction of $Cp_2UNMe$ with $R_2C=O$ , $R = Ph, H$

The initial goal of the computational study is to determine the change in free energy in the irreversible experimental reaction illustrated in eq. 1, where  $Cp$  is the 1,2,4-tri-*t*-butylcyclopentadienyl ligand in the experiment, that is replaced by  $C_5H_5$  in the calculations. The experimental exchange reaction is general, since the arylimido derivatives  $Cp'_2UN(4-(MeO)C_6H_4)$  and  $Cp'_2UN(4-(Me_2N)C_6H_4)$  exchange rapidly with  $Ph_2CO$ , see Experimental section for details.



The reaction illustrated in eq. 1 defines the free energy change and therefore the relative bond dissociation enthalpies of the reactants and products. The calculated  $\Delta G$  for eq. 1 is  $-26 \text{ kcal mol}^{-1}$ , close to the experimental value estimated for the difference between a C=O and a C=NR bond energy.<sup>3,22</sup> In order to calculate the bond dissociation enthalpy of UO relative to UNMe, the free energy for dissociation of  $\text{Ph}_2\text{C}=\text{O}$  into  $\text{Ph}_2\text{C}$  and O (both in their triplet ground states) and  $\text{Ph}_2\text{C}=\text{NMe}$  into  $\text{Ph}_2\text{C}$  and NMe (both in their triplet ground states) is calculated, resulting in a bond dissociation energy for  $\text{Ph}_2\text{C}=\text{O}$  and  $\text{Ph}_2\text{C}=\text{NMe}$  of  $152 \text{ kcal mol}^{-1}$  and  $107 \text{ kcal mol}^{-1}$ , respectively. This results the UO bond dissociation enthalpy that is  $71 \text{ kcal mol}^{-1}$  greater than that of UNMe.<sup>23</sup>

The potential energy surface for the reaction symbolized in eq. 1 is calculated for the reaction in which  $\text{Ph}_2\text{C}=\text{O}$  and  $\text{Ph}_2\text{C}=\text{NMe}$  are replaced by  $\text{H}_2\text{C}=\text{O}$  and  $\text{H}_2\text{C}=\text{NMe}$ , respectively. Figure 1 shows the free energy profile and Figure 2 shows the structures of the extrema. Figure 1 shows that the reaction is exoergic, since  $\Delta G = -34.8 \text{ kcal mol}^{-1}$ , and irreversible. The reaction pathway proceeds by way of adduct formation,  $[\text{U}]\text{NMe}\cdot\text{OCH}_2$ , between the two reactants where [U] is used as a symbol for  $\text{Cp}_2\text{U}$ . In this adduct, the formaldehyde molecule and the NMe fragment are coplanar; rotation of the  $\text{CH}_2$  group around the O-C bond by  $40^\circ$ , so that the p orbital of  $\text{CH}_2$  points towards nitrogen, yields the transition state that is only  $1.2 \text{ kcal mol}^{-1}$  above the adduct. The transition state TS1 connects to a four-center intermediate, which is  $36.3 \text{ kcal mol}^{-1}$  more stable than the separated reactants. The intermediate evolves by crossing a transition state TS2, which is  $14.5 \text{ kcal mol}^{-1}$  above the intermediate. In TS2, the  $\pi$  orbital of the  $\text{H}_2\text{C}=\text{NMe}$  molecule and the U-O fragment are orientated so that the planes defined by the  $\text{CH}_2$  and NUO atoms intersect at an angle of  $139^\circ$ . The transition state TS2 connects to an adduct between  $\text{H}_2\text{C}=\text{NMe}$  and  $\text{Cp}_2\text{UO}$ ,  $[\text{U}]\text{O}\cdot\text{N}(\text{Me})\text{CH}_2$ , which is  $42 \text{ kcal mol}^{-1}$  below the separated reactants. In  $[\text{U}]\text{O}\cdot\text{N}(\text{Me})\text{CH}_2$ , UO and  $\text{N}(\text{Me})\text{CH}_2$  are also coplanar so that the  $\pi$  orbital of the C=N bond does not point towards the UO bond. The free energy of the separated products  $\text{Cp}_2\text{UO}$  and  $\text{H}_2\text{C}=\text{NMe}$  is higher than  $[\text{U}]\text{O}\cdot\text{N}(\text{Me})\text{CH}_2$  by about  $10 \text{ kcal mol}^{-1}$ , in accord with isolation of pyridine adducts in the experimental study.<sup>1</sup> The net reactions are made of a cycloaddition followed by cycloreversion; in the transition state of the cycloaddition the  $\pi$

orbital of H<sub>2</sub>CO is coplanar with the U-NMe bond and in the transition state for cycloreversion the  $\pi$  orbital of H<sub>2</sub>CNMe is coplanar with the U-O bond. In the adducts, [U]NMe•OCH<sub>2</sub> and [U]O•N(Me)CH<sub>2</sub> the  $\pi$  orbitals of the organic molecules are orientated away from the uranium fragment. Thus, the free activation energies of these elementary steps are relatively low since they are associated with bond rotations that do not require significant electronic reorganisation.

The net metathesis of an oxygen atom for a NMe group is exoergic because the UO bond is stronger than that of UNMe. The relatively low activation energies of the two elementary steps calculated for the reaction illustrated in eq 1, in which Ph<sub>2</sub>CO is replaced by H<sub>2</sub>CO, are consistent with the rapid reaction observed in the experimental exchange reaction in which no intermediates are observed in the <sup>1</sup>H NMR spectrum.

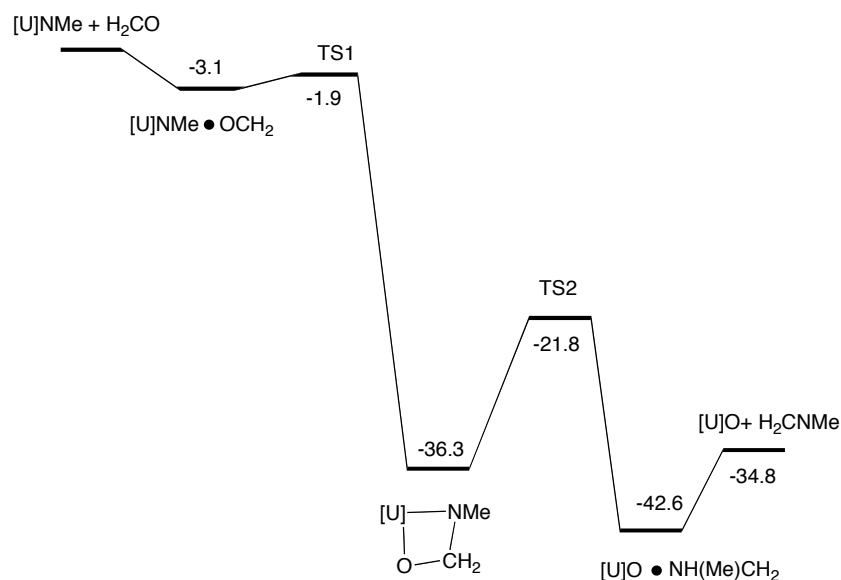


**Figure 1.** Free energy profile ( $\Delta G$ , kcal mol<sup>-1</sup>) for the reaction of Cp<sub>2</sub>UNMe with H<sub>2</sub>C=O to form Cp<sub>2</sub>UO and H<sub>2</sub>C=NMe, [U] = Cp<sub>2</sub>U.

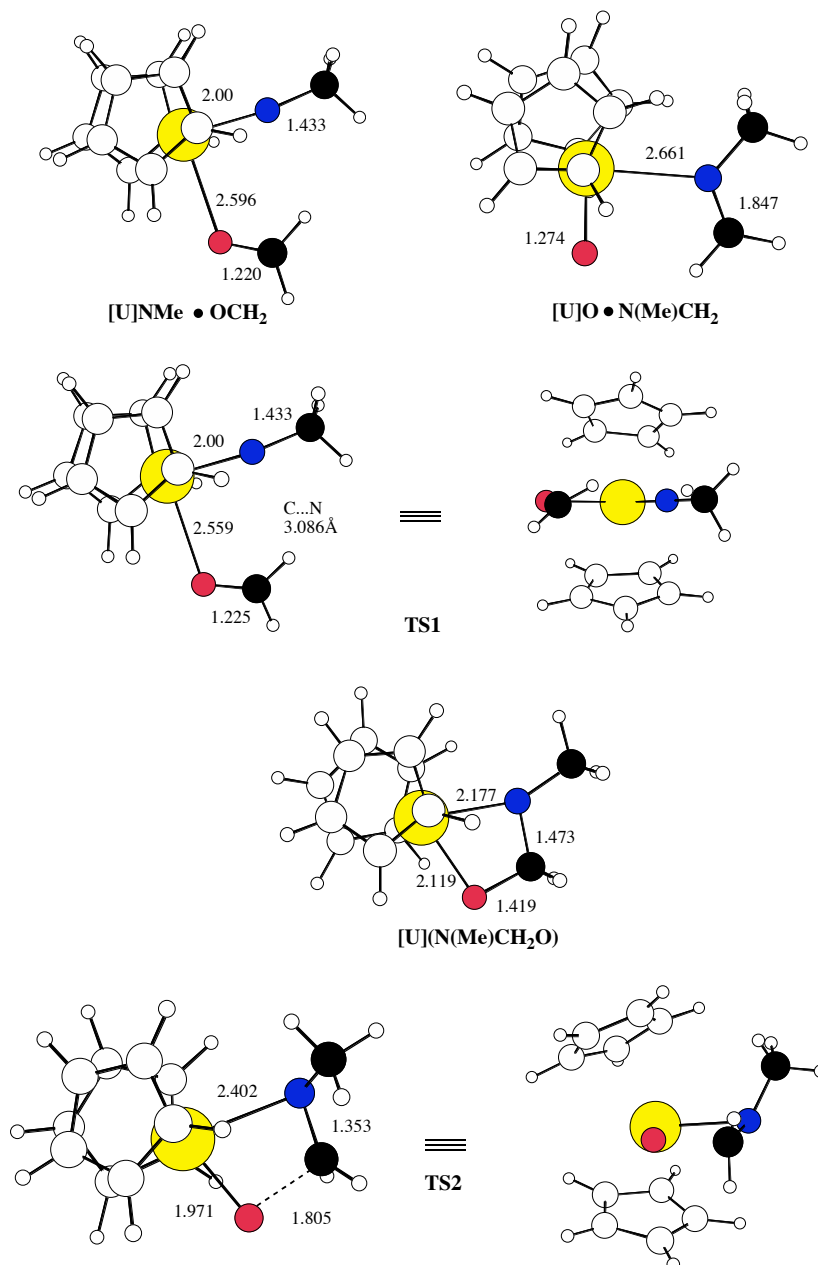
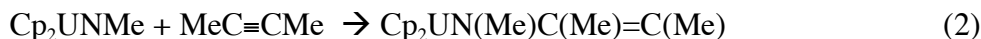


**Figure 2.** Optimized geometries (distances in Å, angle in degrees) for the intermediates and transition states for the reaction of  $\text{Cp}_2\text{UNMe}$  with  $\text{H}_2\text{C}=\text{O}$  to form  $\text{Cp}_2\text{UO}$  and  $\text{H}_2\text{C}=\text{NMe}$ . Two views of the transition states TS1 and TS2 are shown. Black circles are used for the carbon atoms in  $\text{H}_2\text{CO}$  and  $\text{NMe}$ , a red circle is used for oxygen, a blue circle is used for nitrogen, a yellow circle is used for uranium and white circles are used for of the carbon and the hydrogen atoms of the cyclopentadienyl ligand.



## Reaction of Cp<sub>2</sub>UO and Cp<sub>2</sub>UNMe with MeC≡CMe

The calculated free energy profiles for the reactions illustrated in eqs. 2 and 3 are shown in Figure 3. The left-hand side of Figure 3 shows that the transformation in eq. 2 is thermodynamically



favorable ( $\Delta G = -21.5 \text{ kcal mol}^{-1}$ ) and the activation energy is only 11.7 kcal mol<sup>-1</sup> from the separated reactants. These calculated free energies are in agreement with the experimental reaction in which the azametallacycle is isolated and therefore exists as a minimum on the potential energy surface. In solution, the azametallacycle, Cp'<sub>2</sub>UN(Me)C(Me)=C(Me) does not exchange, on the NMR time scale, with added dimethylacetylene or other substituted alkynes showing that the reaction in eq. 2 is not reversible consistent with the calculated values shown in Figure 3. Thus, the reaction between Cp<sub>2</sub>UNMe and MeC≡CMe gives a stable azametallacycle, whose structure, shown in Figure 4, closely resembles that of the isolated metallacycle,<sup>2</sup> which in turn resembles the intermediate in the metathesis reaction illustrated in eq. 1.

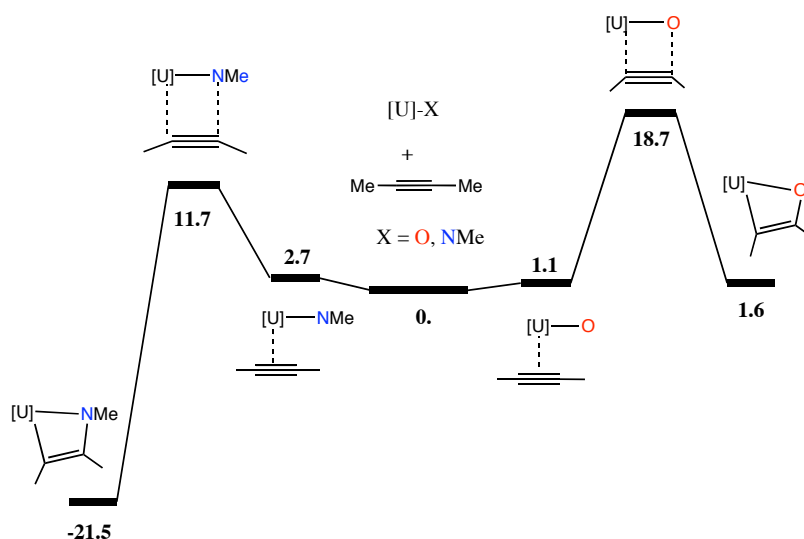


**Figure 3.** Free energy profile ( $\Delta G$  in kcal mol<sup>-1</sup>) for the 1,2 cycloaddition of dimethylacetylene to (a, left-hand side) Cp<sub>2</sub>UNMe and (b, right-hand side) Cp<sub>2</sub>UO, [U] = Cp<sub>2</sub>U.

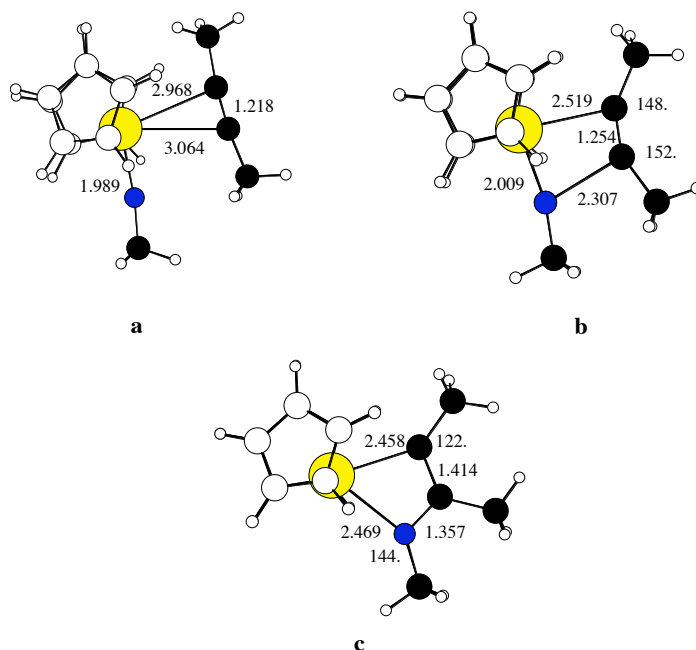


**Figure 4.** Optimized structures of (a) the adduct  $[U]NMe \cdot (MeC \equiv CMe)$ , (b) the transition state for the cycloaddition and (c) the azametallacyclobutene in Figure 3. The color codes for the atoms is identical to that used in Figure 2.

The calculated free energy profile for formation of an oxametallacyclobutane, shown in eq. 3, is illustrated on the right-hand side of Figure 3. The optimized geometries of all extrema are shown in the Figure S1 of the Supporting Information. The calculated free energy change is endoergic, consistent with the experimental result that dimethylacetylene does not react with the oxouranium metallocene even though the activation energy is less than that for the formation of the azametallacyclobutane. This clear cut result is due to the thermodynamic stability of the UO bond relative to that of the UNMe bond.

### Reaction of $Cp_2UO$ and $Cp_2UNMe$ with $H_3SiX$ ( $X = Cl, H$ )

The calculated free energy profiles for the reaction of  $Cp_2UO$  and  $Cp_2UNMe$  with  $H_3SiCl$  is shown in Figure 5. The optimized geometries of all extrema are shown in the Figures S2 and S3 of the Supporting Information. The calculated reaction coordinate shows that both reactions are exoergic

by about  $-30 \text{ kcal mol}^{-1}$ . The activation energies for both reactions are low and the reactions are essentially barrierless. The computational results are surprising since the experimental result is that  $\text{Me}_3\text{SiCl}$  reacts slowly with  $\text{Cp}'_2\text{UO}$  but does not react with  $\text{Cp}'_2\text{UNMe}$  or  $\text{Cp}'_2\text{UN}(4\text{-MeC}_6\text{H}_4)$ . It seems reasonable to suggest that the model calculation in which  $1,2,4\text{-(CMe}_3)_3\text{C}_5\text{H}_2$  is replaced by  $\text{C}_5\text{H}_5$  and  $\text{Me}_3\text{Si}$  by  $\text{H}_3\text{Si}$ , greatly underestimates the steric effects involved in the transition state, that is, as  $\text{Me}_3\text{SiCl}$  approaches the U-NMe fragment, the U-N-Me angle changes from  $180^\circ$  to about  $120^\circ$  as the N-SiMe<sub>3</sub> bond develops. This motion moves the NMe group into the wedge of the  $[\eta^5\text{-}1,2,4\text{-(CMe}_3)_3\text{C}_5\text{H}_2]\text{U}$  fragment, resulting in a transition state whose energy is much higher in the experimental system than in the calculated one.

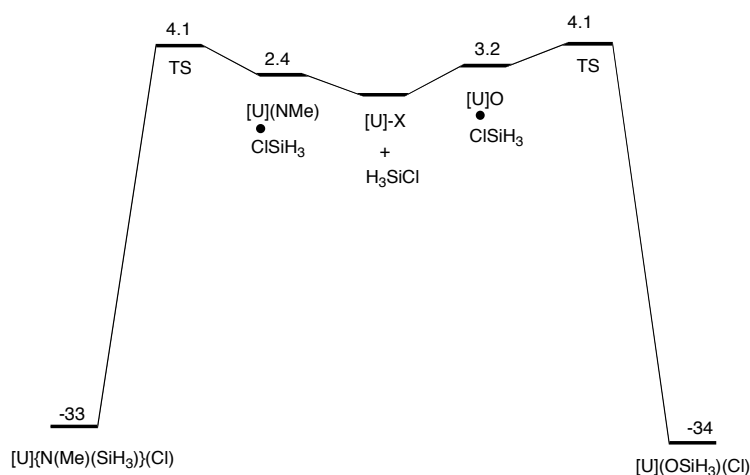


**Figure 5.** Free energy profile ( $\Delta G$  in  $\text{kcal mol}^{-1}$ ) for the 1,2 addition of  $\text{H}_3\text{SiCl}$  to (a, left-hand side)  $\text{Cp}_2\text{UNMe}$  and (b, right-hand side)  $\text{Cp}_2\text{UO}$ ,  $[\text{U}] = \text{Cp}_2\text{U}$ .

The calculated free energy profiles for the reaction of  $\text{SiH}_4$  with either  $\text{Cp}_2\text{UO}$  or  $\text{Cp}_2\text{UNMe}$  (Figures S4 and S5 in the Supporting Information show the geometries of the extrema) show that both reactions are endoergic, since a UH bond is weaker than a UCl bond.<sup>24</sup> Although the reaction with  $\text{SiH}_4$  is not studied experimentally, the reaction of the dihydrogen, which is a useful model for  $\text{SiH}_4$ , does not react with either metallocene derivative.

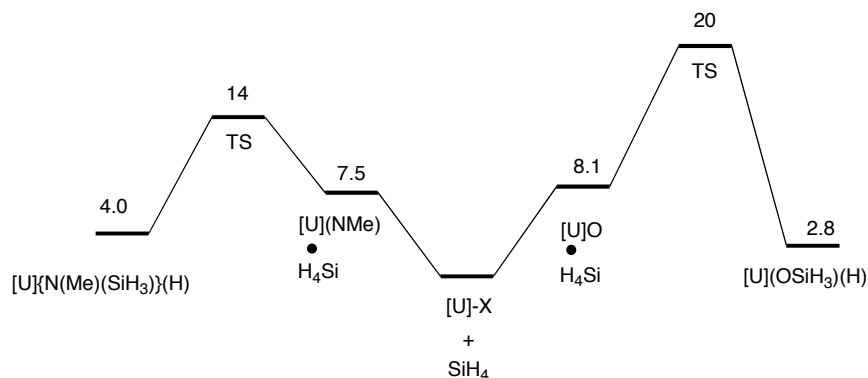


**Figure 6.** Free energy profile ( $\Delta G$  in kcal mol<sup>-1</sup>) for the 1,2 addition of H<sub>4</sub>Si to (a, left-hand side) Cp<sub>2</sub>UNMe and (b, right-hand side) Cp<sub>2</sub>UO, [U] = Cp<sub>2</sub>U.

In summary, all of the calculated potential energy surfaces for these metathesis and addition reactions show that they are under thermodynamic control. Thus, the change in free energy between the initial and final states determines the net chemical reaction and the strength of the UO and UNMe bonds play a critical role. A corollary is that a bond model that describes the ground state electronic structures is essential in order to understand the reactions at the molecular level; such a model is described below.

### Calculated Molecular and Electronic Structure of Cp<sub>2</sub>UX (X = O, NMe) and validation of the DFT calculations.

#### Cp<sub>2</sub>UO

DFT calculations show that the ground state configuration is a triplet and the two unpaired electrons reside in two 5f orbitals. The first singlet state is calculated to be 39 kcal mol<sup>-1</sup> higher in energy at this level of calculation. The DFT optimized geometry of Cp<sub>2</sub>UO in the triplet state is shown as [U]O in Figure 2. The calculated structure can only be compared to that of the 4-dimethylaminopyridine adduct, Cp'<sub>2</sub>UO(4-(Me<sub>2</sub>N)pyridine), because the structure of base-free Cp'<sub>2</sub>UO is unknown. The calculated UO distance of 1.829 Å is close to the experimental value of 1.860(3) Å and the average U-C(Cp) distance of 2.80 Å compares well with the experimental value

of 2.87 Å. The Cp-U-Cp angle of 121° is significantly smaller than the experimental value of 142°, which is expected since C<sub>3</sub>H<sub>5</sub> is sterically smaller than the 1,2,4-tri-*t*-butylcyclopentadienyl ligands in the experimental system. The calculated, unscaled, UO stretching frequency of 811 cm<sup>-1</sup> is in reasonable agreement with the experimental value of 760 cm<sup>-1</sup> found for the pyridine adduct. Thus, the DFT calculation on the model, base-free complex Cp<sub>2</sub>UO reproduces the main geometrical features found in Cp'<sub>2</sub>UO(L). The agreement between the calculated and experimental UO stretching frequencies suggests that the shape of the potential energy surface for the UO bond is not influenced greatly by the presence of the Lewis base and that the UO stretching motion is not strongly coupled to the other stretching motions.

The NBO analysis on Cp<sub>2</sub>UO shows that the uranium and oxygen atoms carry charges of +2.49 on uranium and -1.11 on oxygen; therefore the charge on the Cp<sub>2</sub>U fragment is +1.11 and each Cp-ring carries a charge of -0.7. The charge on U is rather large but significantly smaller than the value implied by the oxidation number. This is in contrast to the charge in, for example Cp<sub>2</sub>CeF or Cp<sub>2</sub>CeOMe, where the charge on Ce is closer to the oxidation number. The lower NBO charge to oxidation number ratio (0.62) in Cp<sub>2</sub>UO, relative to that found in Cp<sub>2</sub>CeF or Cp<sub>2</sub>CeOMe (0.85) corresponds to the traditional view that the bonding in actinide metal compounds utilizes the 5f-electrons whereas the 4f-electrons in the lanthanide metals are essentially core electrons and are little used in 4f-metal to ligand bonds.<sup>25</sup> These two bonding types are usually described by the vague and imprecise terms “covalent” and “ionic” bonding that may be quantitatively expressed by the NBO/oxidation number ratio; the lower the ratio, the more covalent the bond due greater sharing of electrons, or co-valence.

In Cp<sub>2</sub>UO, the NBO charges show that the U-O bond is a σ bond constructed from 80% of the oxygen atom (95%p + 5% s) and 20% from a uranium hybrid orbital largely made from 5f orbitals with a small contribution (8%) from the 6d orbitals. The σ bond is strongly polarized toward the oxygen atom and the other six electrons on oxygen are non-bonding lone pairs, one along and two perpendicular to the U-O axis. The donor-acceptor interaction between the oxygen lone pairs and the

uranium fragment is small since a second order perturbation analysis of the bonding shows that the three lone pairs transfer a total of only 0.2 electrons to uranium. Therefore, the interaction between U and O is a single U-O  $\sigma$  bond polarized toward oxygen and the U-O bond enthalpy results mainly from a Coulombic attraction between the oppositely charged atoms over a short distance augmented by a small orbital contribution, resulting in a small amount of covalence in the bond. This bond model supports the view that the resonance structure  $\text{Cp}_2\text{U}^{(+)}\text{-O}^{(-)}$  dominates  $\text{Cp}_2\text{U=O}$ .

A multi-configurational localized orbital calculation on the DFT optimized geometry supports the model of the U-O bond derived from the DFT calculations. A CAS(2,7) distributing two electrons among the seven 5f orbitals has been carried out. It confirms the triplet nature of the ground state with two unpaired electrons and more importantly shows that this state is properly described by a single reference configuration (85%) with a contribution of only 15% from another configuration, both of which involve only f orbitals. The localized orbitals show the presence of three lone pairs on oxygen and a  $\sigma$  bond between  $\text{Cp}_2\text{U}$  and O. Furthermore, a geometry optimization at the CASSCF level gives a geometry similar to that obtained from the DFT calculations. These results validate the use of DFT for  $\text{Cp}_2\text{UO}$ .

### **$\text{Cp}_2\text{UNMe}$**

The calculated geometrical parameters are in satisfactory agreement with those obtained for  $\text{Cp}'_2\text{U}(\text{N-4-MeC}_6\text{H}_4)$ , since the crystal structure of  $\text{Cp}'_2\text{UNMe}$  is unknown. The calculated U-N distance of 1.982 Å agrees with the experimental value of 1.988(5) Å and the calculated U-N-C(Me) angle of 180° agrees with the experimental value for U-N-C(4-MeC<sub>6</sub>H<sub>4</sub>) of 172.3(5)°.

An NBO analysis gives a charge of +2.38 on U, -0.70 on Cp so that the total negative charge on  $\text{Cp}_2\text{U}$  is +0.99, -1.15 on N and +0.16 on the methyl group so that the total negative charge on the nitrene fragment is -0.99. The NBO charge to oxidation number ratio in the NMe metallocene of 0.60 implies that the UNMe bond is slightly more covalent than the U-O bond, where the ratio is 0.62. This deduction is supported by the NBO analysis, which shows the presence of  $\sigma$ - and  $\pi$ -

bonds; the  $\sigma$  bond is built from 51% of the nitrogen p orbital and 49% of the uranium 5f (97%) and 6d (3%) orbitals. The  $\pi$  bond, which is built from 80% of the nitrogen p orbital and 20% of the uranium 5f (78%) and 6d (22%) orbitals, is polarized towards nitrogen. In addition, second perturbation shows that the lone pair located on nitrogen has 62% s and 38 % p character and this hybridization is different from that used by nitrogen to build the U-N double bond. This lone pair interacts with an empty orbital on uranium made from 7s, 6d and 5f contributions; this delocalization accounts for the linear UNMe geometry.

The multi-configurational, localized-orbital calculation on the geometry optimized from the DFT calculations gives a triplet electronic ground state as in  $\text{Cp}_2\text{UO}$ . The triplet ground state is a combination of two determinants (85% and 15%) as in  $\text{Cp}_2\text{UO}$ . Furthermore the geometry optimization at the CASSCF level gives a geometry identical to that obtained at the DFT level. The localized orbitals show a UN double bond and a lone pair on the NMe fragment. Thus, the bonding picture for the imido metallocenes derived from the DFT agrees with the multi-configurational calculations, which validates the use of DFT calculations for  $\text{Cp}_2\text{UNMe}$ .

CASSCF(2,7) calculations also were carried out on the products of reactions of  $\text{Cp}_2\text{UO}$  with  $\text{SiH}_4$  and  $\text{H}_3\text{SiCl}$  and for  $\text{Cp}_2\text{UNMe}$  with  $\text{SiH}_4$ , all other molecules being too large for a CASSCF calculations. In all cases, a triplet state, dominated by a single configuration was found as the electronic ground state, which validates the use of the DFT method for the potential energy surfaces of the reactions.

### **Comparison of the bonding mode in $\text{Cp}_2\text{UO}$ and $\text{Cp}_2\text{UNMe}$**

Although the NBO charges on the  $\text{Cp}_2\text{U}$  fragments in these two metallocene derivatives are similar, the nature of their chemical bonds is different and the UNMe bond is thermodynamically weaker than the UO bond. In molecular orbital language, the UO bond in  $\text{Cp}_2\text{UO}$  may be formulated by combining the  $\text{Cp}_2\text{U}^{(2+)}$  and  $\text{O}^{(2-)}$  fragments as shown in Figure 7. The U-O bond is largely oxygen in character and the electrons in the  $p_x$  and  $p_y$  orbitals are largely non-bonding. The molecular orbital

description of the UNMe bond is rather different since the orbitals on the NMe<sup>(2-)</sup> fragment are closer in energy to those of the Cp<sub>2</sub>U<sup>(2+)</sup> fragment orbitals; the experimental electron affinity of O is 1.46 eV and that of NMe is 0.02 eV<sup>8</sup> resulting in a UNMe bond that is more covalent.

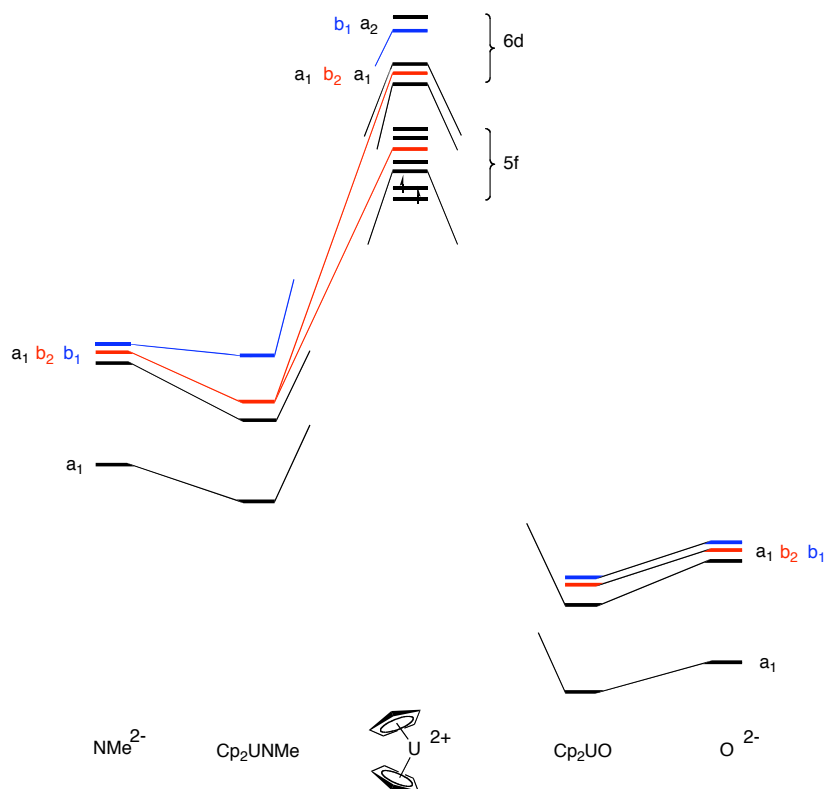


**Figure 7.** Schematic representation of the fragments molecular orbitals of [U], O and NMe, which combine to form [U]O and [U]NMe in  $C_{2v}$  symmetry. Only the metal centered orbitals are shown and all of the orbitals shown for NMe and O are doubly occupied. The absence of correlation lines for the  $b_1$  and  $b_2$  orbitals in the case of oxygen indicates that these oxygen orbitals are non bonding lone pairs.

The bonding in the four-member ring metallacycles formed from the addition of dimethylacetylene to [U]O or [U]NMe, has no remarkable features. The [U]-O and [U]-N bonds are longer than in the corresponding reactants, which weakens them; a similar comment applies to [U](Cl)(OSiH<sub>3</sub>) and [U](Cl){N(Me)(SiH<sub>3</sub>)}.



### **Origin of the reactivity difference between Cp<sub>2</sub>UO and Cp<sub>2</sub>UNMe.**

The reaction of Cp<sub>2</sub>UO and Cp<sub>2</sub>UNMe with dimethylacetylene is the 1,2 addition of a polar U-X bond, in each case, to a non polar triple bond. The UO and UNMe bond can use more than one orbital in the cycloaddition process, and no symmetry restriction governs this process and the reaction cannot be considered forbidden. Accordingly, the activation energies are modest in each case. The difference in the net reactions, *viz.*, Cp<sub>2</sub>UNMe forms a cycloadduct and Cp<sub>2</sub>UO does not, is associated with the net enthalpy changes. The bond analysis of Cp<sub>2</sub>UO shows the presence of a single U-O bond with non bonding lone pairs on oxygen. In contrast, the bond analysis of Cp<sub>2</sub>UNMe shows the presence of a double UNMe bond and a lone pair on the NMe fragment. The calculated heat of reaction between Cp<sub>2</sub>UNMe and Ph<sub>2</sub>CO to form Cp<sub>2</sub>UO and Ph<sub>2</sub>CNMe shows that the UO bond is stronger than the UNMe bond by about 71 kcal mol<sup>-1</sup>. Therefore, it is not surprising that the UO bond is unreactive since it has to overcome this energy penalty.

The reaction of Cp<sub>2</sub>UO or Cp<sub>2</sub>UNMe with H<sub>3</sub>SiCl is a 1,2 addition reaction in which the Si-Cl bond adds to the UO or UNMe fragments. These net reactions are essentially barrierless and equally exoergic, a consequence of the formation of strong U-Cl, UO-Si and UN-Si bonds. The thermochemistry of the 1,2-addition reactions is different from that of the cycloaddition reactions although the two types of reactions proceed through metathesis-like transition states. The experimental outcome of the reaction of Me<sub>3</sub>SiCl with Cp'<sub>2</sub>UO or Cp'<sub>2</sub>UNMe (Cp' = 1,2,4-tri-*t*-butylcyclopentadienyl) is however different from the calculational outcome, since although Cp'<sub>2</sub>U(OSiR<sub>3</sub>)Cl forms and Cp'<sub>2</sub>UN(SiR<sub>3</sub>)Cl does not, a result most reasonably ascribed to steric effects. In the case of SiH<sub>4</sub>, the calculations indicate that the reaction with Cp<sub>2</sub>UO and Cp<sub>2</sub>UNMe is endoergic, the result of the weaker UH bond relative to a UCl bond.

### **Summary**

The calculated free energy profiles for the reaction between Cp<sub>2</sub>UNMe with ketones and acetylenes and Cp<sub>2</sub>UO with silylhalides show that the reactions are under thermodynamic control

since the reactions proceed with modest activation free energies. The calculated results mirror the experimental results for [1,2,4-(CMe<sub>3</sub>)<sub>3</sub>C<sub>5</sub>H<sub>2</sub>]<sub>2</sub>UNMe with benzophenone and dimethylacetylene and for [1,2,4-(CMe<sub>3</sub>)<sub>3</sub>C<sub>5</sub>H<sub>2</sub>]<sub>2</sub>UO with Me<sub>3</sub>SiCl. The origin of the reactivity differences is traced to the strength of the UO bond relative to that of the UNMe bond. The stronger UO bond is not a “double bond” but it is a strongly polarized one in which the dominant resonance structure is Cp<sub>2</sub>U<sup>(+)</sup>-O<sup>(-)</sup>, presumably due to the large electronegativity of the oxygen atom. On the other hand, the thermodynamically weaker UNMe bond has more “double bond” character, the net result of the lower electronegativity of the NMe group. Thus, these bonds display different reactivity patterns because of their different bond strengths and these differences are not related to the multiple bond character.

## **Experimental Details**

The experimental studies were carried out as previously described.<sup>1,2</sup> The reaction of Cp'<sub>2</sub>UNMe, Cp'<sub>2</sub>UO, or Cp'<sub>2</sub>UO(4-(Me<sub>2</sub>N)C<sub>6</sub>H<sub>4</sub>) in presence of BPh<sub>3</sub>, with dihydrogen or dideuterium was carried out in a sealed NMR tube at 1 atm total pressure in C<sub>6</sub>D<sub>6</sub>.

**Reaction of [η<sup>5</sup>-1,2,4-(CMe<sub>3</sub>)<sub>3</sub>C<sub>5</sub>H<sub>2</sub>]<sub>2</sub>UN(4-(MeO)C<sub>6</sub>H<sub>4</sub>) with Ph<sub>2</sub>CO. NMR Scale.** To an NMR tube charged with [η<sup>5</sup>-1,2,4-(CMe<sub>3</sub>)<sub>3</sub>C<sub>5</sub>H<sub>2</sub>]<sub>2</sub>UN(4-(MeO)C<sub>6</sub>H<sub>4</sub>) (17 mg, 0.02 mmol) and C<sub>6</sub>D<sub>6</sub> (0.5 mL) was added benzophenone (3.6 mg, 0.02 mmol). The color of the solution immediately changed from dark brown to brown-red. The <sup>1</sup>H NMR spectrum contained resonances due to [η<sup>5</sup>-1,2,4-(CMe<sub>3</sub>)<sub>3</sub>C<sub>5</sub>H<sub>2</sub>]<sub>2</sub>UO and Ph<sub>2</sub>C=N-4-(MeO)C<sub>6</sub>H<sub>4</sub><sup>26</sup> (<sup>1</sup>H NMR (C<sub>6</sub>D<sub>6</sub>): δ 7.94 (m, 2H, aryl *H*), 7.03-6.87 (m, 8H, aryl *H*), 6.74 (m, 1H, aryl *H*), 6.57 (m, 1H, aryl *H*), 6.37 (m, 2H, aryl *H*), 3.45 (s, 3H, CH<sub>3</sub>)) (100% conversion relative to an internal standard).

**Reaction of [η<sup>5</sup>-1,2,4-(CMe<sub>3</sub>)<sub>3</sub>C<sub>5</sub>H<sub>2</sub>]<sub>2</sub>UN(4-(Me<sub>2</sub>N)C<sub>6</sub>H<sub>4</sub>) with Ph<sub>2</sub>CO. NMR Scale.** To an NMR tube charged with [η<sup>5</sup>-1,2,4-(CMe<sub>3</sub>)<sub>3</sub>C<sub>5</sub>H<sub>2</sub>]<sub>2</sub>UN(4-(Me<sub>2</sub>N)C<sub>6</sub>H<sub>4</sub>) (18 mg, 0.02 mmol) and C<sub>6</sub>D<sub>6</sub> (0.5 mL) was added benzophenone (3.6 mg, 0.02 mmol). The color of the solution immediately changed from dark brown to brown-red. The <sup>1</sup>H NMR spectrum contained resonances due to [η<sup>5</sup>-1,2,4-

(CMe<sub>3</sub>)<sub>3</sub>C<sub>5</sub>H<sub>2</sub>I<sub>2</sub>UO and Ph<sub>2</sub>C=N-4-(Me<sub>2</sub>N)C<sub>6</sub>H<sub>4</sub><sup>27</sup> (<sup>1</sup>H NMR (C<sub>6</sub>D<sub>6</sub>): δ 7.92 (m, 2H, aryl *H*), 6.97 (m, 6H, aryl *H*), 6.84 (m, 2H, aryl *H*), 6.71 (m, 1H, aryl *H*), 6.55 (m, 1H, aryl *H*), 6.37 (m, 2H, aryl *H*), 3.19 (s, 6H, CH<sub>3</sub>)) (100% conversion relative to an internal standard).

## Computational Details

The Stuttgart-Dresden-Bonn small core Relativistic Effective Core Potential (RECP) has been used to represent the 78 core electrons of U, leaving 14 valence electrons in the 6s, 6p, 5f, 6d, and 7s shells.<sup>28</sup> The associated basis set, including up to g functions, has been used to represent the valence orbitals. C, N, O and H have been represented by an all-electron 6-31G(d, p) basis set.<sup>29</sup> Si and Cl atoms were also treated with a large core RECP in combination with the adapted basis set,<sup>30</sup> augmented by a polarization d function (Si, exp = 0.284), Cl exp = 0.643.<sup>31</sup> Calculations have been carried out at the DFT(B3PW91) level<sup>32</sup> with Gaussian 03.<sup>33</sup> The nature of the extrema (minimum or transition state) has been established with analytical frequency calculations and the intrinsic reaction coordinate (IRC) has been followed to confirm that transition states connect to reactants and products. The zero point energy (ZPE) and entropic contribution have been estimated within the harmonic potential approximation. The Gibbs free energy, ΔG, was calculated for T = 298.15K and 1 atm. The NBO analysis was carried out.<sup>34</sup>

The validity of the DFT approach was determined by a wave function based method. The SCF calculations were carried out with the MOLCAS 6 suite of programs<sup>35</sup> and the subsequent CASSCF calculations with localized orbitals were performed with the NOSCF program.<sup>36</sup> In these calculations the U atom was treated with an *ab-initio* model potential (AIMP)<sup>37</sup> including 78 electrons in core with the associated basis sets. The C, N O and H atoms were represented with ANO type basis sets.<sup>38</sup> The CASSCF(2,7) calculations, carried out on the DFT optimized geometry, revealed that two configurations had to be considered. Consequently the geometry optimization at the CAS level was carried out for a CASSCF(2,2) for selected cases.

**Supplementary Information:** Optimized geometries of the intermediates and transition states for the reactions of Cp<sub>2</sub>UO and MeC≡CMe (Figure S1), Cp<sub>2</sub>UO and H<sub>3</sub>SiCl (Figure S2), Cp<sub>2</sub>UMe and H<sub>3</sub>SiCl (Figure S3), Cp<sub>2</sub>UO and SiH<sub>4</sub> (Figure S4), Cp<sub>2</sub>UMe and SiH<sub>4</sub> (Figure S5). Full list of authors for Gaussian 03. List of coordinates, Energy and free energy of all optimized species.

**ACKNOWLEDGMENT:** This work was partially supported by the Director Office of Energy Research Office of Basic Energy Sciences, Chemical Sciences Division of the U. S. Department of Energy under Contract No DE-AC02-05CH11231. Calculations were in part carried out on the national computing centre CINES and CALMIP (France). N.B. thanks the Commissariat à l'Énergie Atomique (CEA), France for funding. O.E. thanks the Miller Institute for a Visiting Miller Professorship at U.C. Berkeley. The French authors thank the CNRS, notably the PICS 3422, and the Ministère of National Education for funding.

#### References

- (1) Zi, G.; Jia, L.; Werkema, E.L.; Walter, M. D.; Gottfriedsen, J. P.; Andersen, R. A. *Organometallics* **2005**, *24*, 4251.
- (2) Zi, G.; Blosch, L. L.; Jia, L.; Andersen R. A. *Organometallics* **2005**, *24*, 4602.
- (3) Coates, G. E.; Sutton L. E. *J. Chem. Soc.* **1948**, 1187.
- (4) Straub, T.; Haskel, A.; Neyroud, T. G.; Kapon, M.; Botoshansky, M.; Eisen, M. S. *Organometallics* **2001**, *20*, 5017.
- (5) Blondel, C. *Phys. Scr.* **1995**, *58*, 31.
- (6) Travers, M. J.; Cowles, D. C.; Clifford, E. P.; Ellison, G. B. *J. Am. Chem. Soc.* **1992**, *114*, 8699. Borden, W. T.; Gritsan, N. P.; Hadad, C. M.; Karney, W. L.; Kemnitz, C. R.; Platz, M. S. *Acc. Chem. Res.* **2000**, *33*, 765.
- (7) Neumark, D.M.; Lykke, K. R.; Andersen, T.; Lineberger, W. C. *Phys. Rev. A* **1985**, *32*, 1890.
- (8) Travers, M. J.; Cowles, D. C.; Clifford, E. P.; Ellison, G. B.; Engelking, P. C. *J. Chem. Phys.* **1999**, *111*, 5349.

- (9) Pepper, M.; Bursten, B. E. *Chem. Rev.* **1991**, *91*, 719. Cao, X.; Dolg, M. *Coord. Chem. Rev.* **2006**, *250*, 900. Vallet, V.; Macak, P.; Wahlgren, U.; Grenthe, I. *Theor. Chem. Acc.* **2006**, *115*, 145. Kaltsoyannis, N. *Chem. Soc. Rev.* **2003**, *32*, 9. Hay, P. J. *Farad. Disc.* **2003**, *124*, 69. Kaltsoyannis, N.; Hay, P.J.; Jun, L.; Blaudeau, J.-P.; Bursten in *The Chemistry of the Actinide and Transactinide Elements*, Morss, L. R.; Edelstein, N. M. ; Fuger, J. ; Katz , J. J. Eds 3<sup>rd</sup> Ed. 2006, Springer , Chapter 17.
- (10) Pyykkö, P. *Relativistic Theory of Atoms and Molecules* 1915-RATM data base. Version 11.0, 2005. [www.csc.fi/rtam](http://www.csc.fi/rtam).
- (11) Pyykkö, P. *Inorg. Chim. Acta* **1987**, *139*, 989.
- (12) Vallet, V.; Schimmelpfennig, B.; Maron, L.; Teichteil, C.; Leininger, T.; Gropen, O.; Grenthe, I.; Wahlgren, U. *Chem. Phys.* **1999**, *244*, 185.
- (13) Vallet, V.; Maron, L.; Schimmelpfennig, B.; Leininger, T.; Teichteil, C.; Gropen, O.; Grenthe, I.; Wahlgren, U. *J. Phys. Chem. A* **1999**, *103*, 9285.
- (14) Dolg, M.; Fulde, P.; Stoll, H.; Preuss, H.; Chang, A.; Pitzer, R. M. *Chem. Phys.* **1995**, *195*, 71.
- (15) Maron, L.; Leininger, T.; Schimmelpfennig, B.; Vallet, V.; Heully, J.-L.; Teichteil, C.; Gropen, O.; Wahlgren, U. *Chem. Phys.* **1999**, *244*, 195.
- (16) Wang, W.; Andrews, L.; Li, J.; Bursten, B. E. *Angew. Chem. Int. Ed.* **2004**, *43*, 2554. Ismail, N.; Heully, J.-L.; Saue, T.; Daudey, J.-P.; Marsden, C. J. *Chem. Phys. Lett.* **1999**, *300*, 296.
- (17) See for instance, van Besien, E.; Pierloot, K.; Gorlier-Walrand, C. *Phys. Chem. Chem. Phys.* **2006**, 4311. Denning, R. G.; Green, J. C.; Hutchings, T. E.; Dallera, C.; Tagliaferri, A.; Giarda, K.; Brookes, N. B.; Braicovich, L. J. *J. Chem. Phys.* **2002**, *117*, 8008. Szabo, Z.; Toraishi, T.; Valet, V.; Grenthe, I. *Coord. Chem. Rev.* **2006**, *250*, 784.
- (18) Belkiri, L.; Lissillour, R.; Boucekkine, A. *J. Mol. Struct. Theochem.* **2005**, *757*, 155. Hayton, T. W.; Boncella, J. M.; Scott, B. L. Palmer, P. D.; Batista, E. R.; Hay, P. J. *Science* **2005**, *310*, 1941. Hayton, T. W.; Boncella, J. M.; Scott, B. L.; Batista, E. R.; Hay, P. J. *J. Am. Chem. Soc.* **2006**, *128*, 10549.
- (19) Zachmanoglou, C. E.; Docrat, A.; Bridgewater, B. M.; Parkin, G.; Brandow, C. G.; Bercaw, J. E.; Jardine, C. N.; Lyall, M.; Green, J. C.; Keister, J. B. *J. Am. Chem. Soc.* **2002**, *124*, 9525. Conejo, M. D.; Parry, J. S.; Carmona, E.; Schultz, M.; Brennan, J. G.; Beshouri, S. M.; Andersen, R. A.; Rogers, R. D.; Coles, S.; Hursthouse, M. *Chem. Eur. J.* **1999**, *5*, 3000.

- (20) Maron, L.; Werkema, E. L.; Perrin, L.; Eisenstein, O.; Andersen, R. A. *J. Am. Chem. Soc.* **2005**, *127*, 279. Werkema, E. L.; Messines, E.; Perrin, L.; Maron, L.; Eisenstein, O.; Andersen, R. A. *J. Am. Chem. Soc.* **2005**, *127*, 7781. Sherer, E. C.; Cramer, C. J. *Organometallics* **2003**, *22*, 1682. Perrin, L.; Maron, L.; Eisenstein, O. *New J. Chem.* **2004**, *10*, 1255. Barros, N.; Eisenstein, O.; Maron, L. *Dalton Trans.* **2006**, 3052.
- (21) Kanellakopoulos, B. in *Organometallics of the f Elements* Marks T. J. Fisher, R. D. Eds D. Riedel, Dordrecht, Holland 1978, pp 1-36. Lukens, W. W.; Beshouri, S. M.; Blossch, L. L. Stuart, A. L.; Andersen R. A. *Organometallics* **1999**, *18*, 1235.
- (22) Sandorfy, C. In *The chemistry of the C-N Double Bond* Patai, S. Ed. Interscience: London, 1970; Chapter 1.
- (23)  $\Delta H(\text{reaction})$  for eq 1 =  $\{\text{Cp}_2\text{U}\}\{\text{O}\} + \{\text{Ph}_2\text{C}\}\{\text{NMe}\} - (\{\text{Cp}_2\text{U}\}\{\text{NMe}\} + \{\text{Ph}_2\text{C}\}\{\text{O}\})$  where the brackets indicate the chemical fragments involved in the calculation of the bond dissociation energies. Replacing  $\Delta H(\text{reaction})$ ,  $\{\text{Ph}_2\text{C}\}\{\text{NMe}\}$  and  $\{\text{Ph}_2\text{C}\}\{\text{O}\}$  by the values -26, 107 and 152 kcal mol<sup>-1</sup> respectively yields the difference  $\{\text{U}\}\{\text{O}\} - (\{\text{U}\}\{\text{NMe}\}) = 71$  kcal mol<sup>-1</sup>.
- (24) Bruno, J. W.; Stecher, H. A.; Morss, L. R.; Sonnenberger, D. C.; Marks, T. J. *J. Am. Chem. Soc.* **1986**, *108*, 7275. Jemine, X.; Goffart, J.; Berthet, J. C.; Ephritikhine, M. *J. C. S. Dalton Trans.* **1992**, 2439. Leal, J. P.; Marques, N.; Pires de Matos, A.; Calhorda, M. J.; Galvao, A. M.; Martinho Simoes, J. A. *Organometallics* **1992**, *11*, 1632. Martinho Simoes, J. A.; Leal, J. P. *ChemTracks, Inorg. Chem.* **1991**, *3*, 143. Leal, J. P.; Marques, N.; Takats J. *J. Organomet. Chem.* **2001**, *632*, 209.
- (25) (a) The first indication of covalency in the 5f block metals was the observation of <sup>19</sup>F superhyperfine splitting in the EPR spectrum of U(III) atoms in CaF<sub>2</sub>. Bleaney, B.; Llewellyn, P. M.; Jones, D. A. *Proc. Phys. Soc.* **1956**, *B69*, 858. (b) Maron, L.; Eisenstein, O. *J. Phys. Chem. A* **2000**, *104*, 7140.
- (26) Okubo, M.; Ueda, S. *Bull. Chem. Soc. Jpn.* **1980**, *53*, 281.
- (27) Henderson, W. A.; Zweig, A. *Tetrahedron* **1971**, *27*, 5307.
- (28) <http://www.theochem.uni-stuttgart.de/pseudopotentiale/clickpse.en.html>.
- (29) Hariharan, P. C.; Pople, J. A. *Theor. Chim. Acta* **1973**, *28*, 213.
- (30) Bergner, A.; Dolg, M.; Kuchle, W.; Stoll, H.; Preuss, H. *Mol. Phys.* **1993**, *80*, 1431.
- (31) Maron, L.; Teichteil, C. *Chem. Phys.* **1998**, *237*, 105.

- (32) Perdew, J. P.; Wang, Y. *Phys. Rev. B* **1992**, *45*, 13244. Becke, A. D. *J. Chem. Phys.* **1993**, *98*, 5648. Burke, K.; Perdew, J. P.; Yang, W. in “*Electronic Density Functional Theory: Recent Progress and New Directions*”; Dobson, J. F.; Vignale, G., Das, M. P. Eds. **1998**, Plenum.
- (33) Gaussian 03, Revision C.02, Pople, J. A. *et al.*
- (34) Reed, A. E.; Curtiss, L. A.; Weinhold, F. *Chem. Rev.* **1988**, *88*, 899.
- (35) Karlström, G.; Lindh, R.; Malmqvist, P.-Å.; Roos, B. O.; Ryde, U.; Veryazov, V.; Widmark, P.-O.; Cossi, M.; Schimmelpfennig, B.; Neogrady, P.; Seijo, L. *Computational Material Science*, **2003**, *28*, 222 [<http://www.teokem.lu.se/molcas/documentation/manual/node85.html#Karlstroem:03a>].
- (36) Maynau, D.; Evangelisti, S.; Guihery, N.; Calzado, C. J.; Malrieu, J.-P. *J. Chem. Phys.* **2002**, *116*, 10060.
- (37) Seijo, L.; Barandiaran, Z.; Harguindey, E. *J. Chem. Phys.* **2001**, *114*, 118.
- (38) Widmark, P.-O.; Malmqvist, P.-A.; Roos, B. O. *Theor. Chim. Acta* **1990**, *77*, 291.

